Volume 25
Number 2

December *2023*
(ISSN 1109-1606)

Journal of

APPLIED ELECTROMAGNETISM

JAE

Institute of Communication and Computer Systems

Athens - GREECE

Volume 25 **December 2023**
Number 2 **(ISSN 1109-1606)**

JOURNAL
OF
APPLIED ELECTROMAGNETISM

Institute of Communication and Computer Systems

Athens - GREECE

Volume 25 **Number 2**

December 2023

TRANS BLACK SEA REGION UNION OF APPLIED ELECTROMAGNETISM (BSUAE)

JOURNAL OF APPLIED ELECTROMAGNETISM

Institute of Communication and Computer Systems

Athens - GREECE

Publishing Department

Journal of Applied Electromagnetism

Copyright Form

The undersigned I confirm that I agree the publication of the article

in the Journal of Applied Electromagnetism and the copyright to belong to Trans Black Sea Union of Applied Electromagnetism. I understand that I have the full right to reuse this manuscript for my own purposes.

Name:

Surname:

Address:

E-mail:

Signed:

***Please send the previous form signed either by e-mail to pfrangos@central.ntua.gr , or by fax to the fax number: +30 210 772 2281, attention of Prof. P. Frangos.**

Address

Institute of Communication and Computer Systems,

National Technical University of Athens,

9, Iroon Polytechniou Str.,

157 73 Athens - GREECE

Tel: (+30) 210 772 3694

Fax: (+30) 210 772 2281, attention of Prof. P. Frangos

e-mail: pfrangos@central.ntua.gr

Web site: **http://jae.ece.ntua.gr**

TRANS BLACK SEA REGION UNION OF APPLIED ELECTROMAGNETISM (BSUAE)

JOURNAL OF APPLIED ELECTROMAGNETISM (JAE)

Volume 25 Number 2 December 2023

CONTENTS

The thermal effects caused by exposure to the electromagnetic (EM) field emitted by the mobile phone antenna have been investigated in the presented paper. A novelty is to study matching of the mobile phone dipole antenna to the free space for the case of a non-homogenous child model with different hand positions and different distances (1mm, 10mm, 20mm) of the mobile phone (with and without hand) from the child's head model; Through computer modeling (using the Finite-Difference Time-Domain (FDTD) method) have been evaluated the EM field energy absorption power by the child model considering the hand influence (holding the mobile phone) and have been conducted a comparative analysis for hand free cases. Because the hand holding the phone absorbs most of the radiation energy emitted by the mobile phone antenna. Studied the dependence of SAR (specific absorption rate SAR-W/kg) on the conditions of matching of the mobile phone antenna with the free space. Developed recommendations for the correct use of a mobile phone to reduce the reactive field near the child head in order to reduce head SAR values. The results of the study are presented below.

The analysis of digital images having complex structure includes the application both processing methods and mathematical algorithms. As a rule, the processing helps to find the representation of an image which is more suitable for application of mathematical methods. Depending on the type of images the obtaining of an appropriate presentation may be the essential part of the study. In the paper we apply the application of fractal and multifractal methods to compare crystals of medical preparations with a control image which does not contain a preparation (placebo).The images under study were prepared for analysis by a special program and transformed to grayscale palette. For

several classes containing 5-6 images the applied methods demonstrated the separation of obtained characteristics, which means the difference in structures of medical preparations and placebo.

EVALUATION OF THE MOBILE PHONE ANTENNA ELECTROMAGNETIC FIELD THERMAL EFFECTS FOR THE NONHOMOGENEOUS CHILD MODEL BY USING COMPUTER SIMULATION

(selected from CEMA'23 Conference)

Tamar Nozadze[*], Mtvarisa Kurtsikidze[**] and Giorgi Ghvedashvili[*]

[*] Ivane Javakhishvili Tbilisi State University, Department of Electric and Electronic Engineering, Laboratory of Applied Electrodynamics and Radio Engineering,
3, Chavchavadze Ave. 0176, Tbilisi, Georgia

[**] Samtskhe-Javakheti State University,
113 Shota Rustaveli St, Akhaltsikhe, Georgia

E-mail: tamar.nozadze@tsu.ge

Abstract

The thermal effects caused by exposure to the electromagnetic (EM) field emitted by the mobile phone antenna have been investigated in the presented paper. A novelty is to study matching of the mobile phone dipole antenna to the free space for the case of a non-homogenous child model with different hand positions and different distances (1mm, 10mm, 20mm) of the mobile phone (with and without hand) from the child's head model; Through computer modeling (using the Finite-Difference Time-Domain (FDTD) method) have been evaluated the EM field energy absorption power by the child model considering the hand influence (holding the mobile phone) and have been conducted a comparative analysis for hand free cases. Because the hand holding the phone absorbs most of the radiation energy emitted by the mobile phone antenna. Studied the dependence of SAR (specific absorption rate SAR-W/kg) on the conditions of matching of the mobile phone antenna with the free space. Developed recommendations for the correct use of a mobile phone to reduce the reactive field near the child head in order to reduce head SAR values. The results of the study are presented below.

1. INTRODUCTION AND PROBLEM FORMULATION

Technological progress has influenced into all areas of human life. Communications and other electrical devices are sources of radiofrequency (RF) and

microwave (MW) electromagnetic (EM) radiation. The natural sources of EM field are the sun, stars and others. The human body and living organisms is adapted to the natural environment created by them. Sources of EM field are also electrical devices, the EM fields emitted by which cause "pollution" of this natural EM background. Therefore, it is very important to study the background generated by base stations and different types of EM emitters. It is also important to study the impact of the EM field on humans, living organisms in nature and the environment in various cases, which can significantly change the existing natural EM background. The influence of electromagnetic fields (EM) emitted by mobile phone antennas on human, has been studied for many years before and especially after widespread introduction and use of cellular communications technology. Since exposure to EMF increases with reduced distance between the emitting antennas and the user the efforts to minimize exposure while increasing the radiated power are one of the most important tasks to enable efficient communication systems that are at the same time complaint with international safety standard on human exposure to EM field [1]-[3].

SAR is used for evaluating the RF radiation characteristics of mobile phones to determine if they meet Federal Communications Commission (FCC) safety requirements [4]. Current safety standards, guidelines set maximum radiation levels based on the amount of energy absorbed by the human body emitted by cell phones during communication. There are concerns that exposure to EM fields emitted by cell phones can cause cancer and other potential health problems. In 2011, the World Health Organization [5] and the International Agency for Research on Cancer [6] reviewed several scientific studies and based on the results of the studies, they classified mobile phones as a possible human carcinogen, putting them in the same category as lead, gasoline engine exhaust and chloroform.

The energy absorption in the human head caused by the exposure of human to the EM field of a mobile phone antenna depends on many factors. The distance from the antenna, the power and frequency of the radiated source, and the position of the hand are also very important [7]-[10]. In addition, the type of antenna, the shape and material of the mobile "case", the location of the phone, the anatomy of the human head and the dielectric properties of the tissue significantly affect the absorption of field energy. Existing safety standards, which have not been updated in recent decades, determine the level of radiation

for cases that pose a threat to human health. On the other hand, there may be some biological effects, but they are not considered dangerous for humans [11]. Harmful effects on children are very important. They are exposed to radio-frequency radiation from an early age. Main target for radiation is their brain, the skull is much thinner than adults are, and therefore the possible negative impact on children can be more serious [11].

Mobile phone antennas are designed by mobile phone manufacturers so to have as low losses as possible and radiate most of the power delivered to the antenna. In this case, the antenna is well matched with free space. A quantitative characteristic is the S11 reflection coefficient, or S11 parameter. Relative positions of the user's head, hand and fingers influence on the values of the S11 parameter. Manufacturers do not consider this important factor in the process of manufacturing/testing mobile phones.

During mobile telephone communication, the antenna, the user's hand and head are mainly involved in the formation of radiation. A reactive EM field is often created near the human head. Therefore, the aim of the presented research is to study in detail how different hand configuration and different distances between the child head and the phone affect the mobile phone antenna parameter value (S11 coefficient).

The goal of the study is to determine the correlation between the matching parameter of the phone antenna (S11) and the EM field energy (SAR) absorbed by human tissues for 2100 MHz frequency, considering that smartphones automatically increase the radiation power to achieve a reliable connection in case of weak signal to the base station.

2. MATERIALS AND METHOD

Research was conducted through computer modeling. The numerical simulations were carried out using the FDTDLab software package developed at TSU [7]-[10]. The FDTDLab program is based on the Finite-Difference Time-Domain (FDTD) method, which is a discretization of Maxwell's equations. A discrete grid, each cell of which is 1mm, is considered for the calculation area. A three-dimensional inhomogeneous discrete model of the child (Thelonious) from the "virtual population" (IT‟IS Foundation) [12] with 1mm discretization was used for numerical calculations Figure 1, Figure 2.

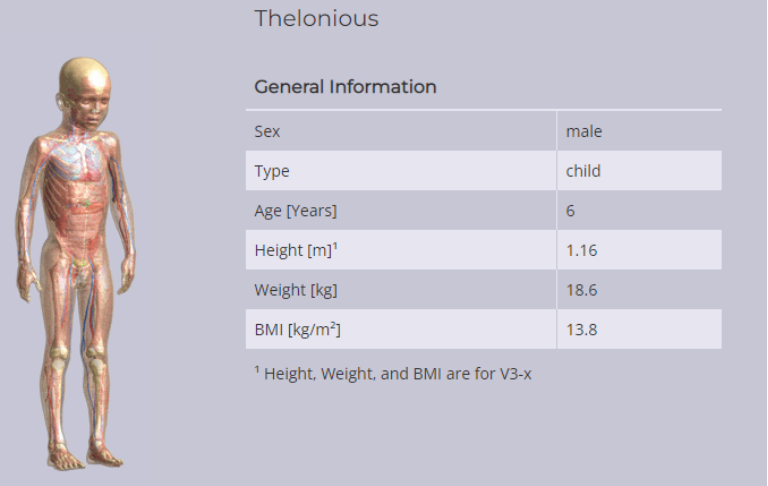

a)

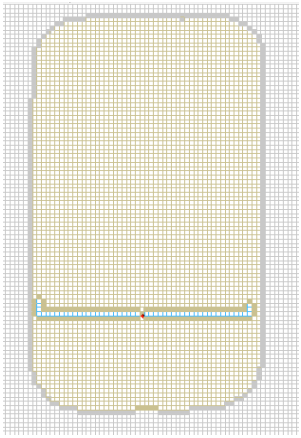

b)

Figure 1. a) Physical data of the child model (Thelonious). b) Mobile phone discrete model with dipole antenna.

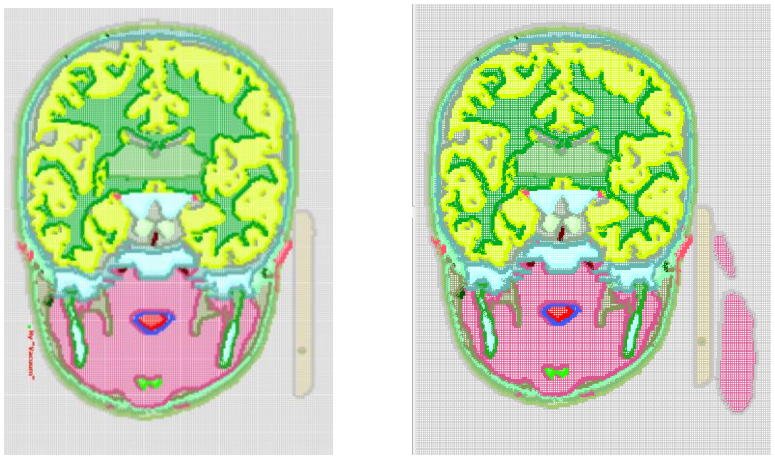

a) b)

Figure 2. Child discrete head models with the mobile phone: a) without hand, b) with hand.

Frequency-dependent tissue parameters were used from the known database [13], a sinusoidal waveform of 2100 MHz frequency will be used for simulations.

The dipole length for the selected frequency (2100 MHz) was selected so the S11 coefficient to be the lowest as possible. In this case, the best antenna matching to open space was obtained. The length of the dipole antenna was 0.52 mm.

One hand position was prepared for the child's model (because the child's hand is approximately the size of a mobile phone). The mobile phone and the hand were placed at distances of 1mm, 10mm and 20mm from the child head model.

3. RESULTS AND DISCUSSIONS

On Figure 3 it is shown frequency characteristics for a considered mobile phone dipole antenna for the selected frequency.

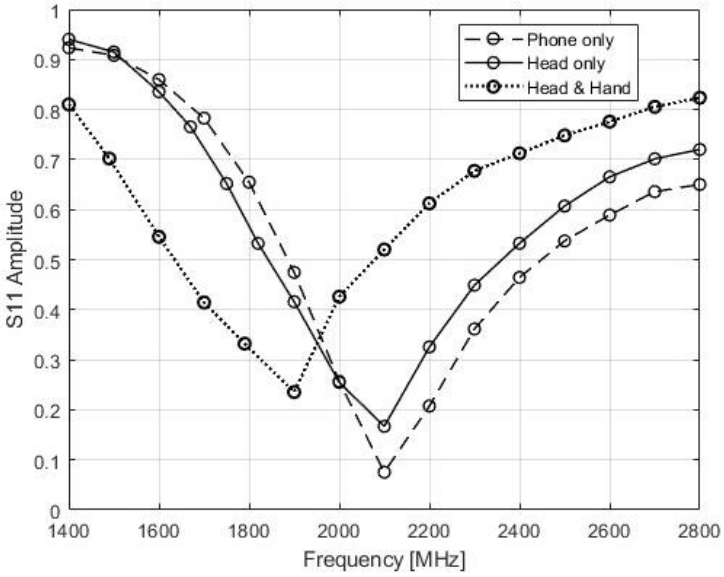

Figure 3. Mobile phone dipole antenna frequency characteristics.

As the numerical experiments show, the values of the S11 coefficient increase due to the influence of the hand. In some cases, the head, hand reduce the S11 coefficient, this means that the antenna is well matched to the free space, not at the considered frequency, but at shifted frequencies. It also depends on the modeling scenarios.

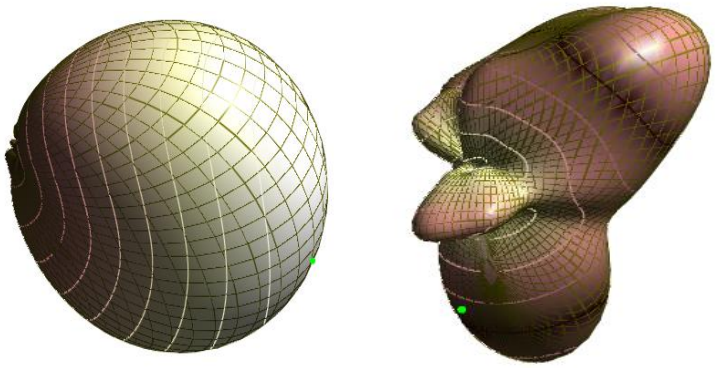

a) b)

Figure 4. 3D radiation patterns for the mobile antenna at 2100 MHz: a) head model only, b) head with hand

Three-dimensional radiation patterns of a mobile phone antenna without head and with hand are shown in Figure 4. The obtained results show that when the presence of hand and head is considered, the radiation pattern and re-radiation power in the far zone are changed;

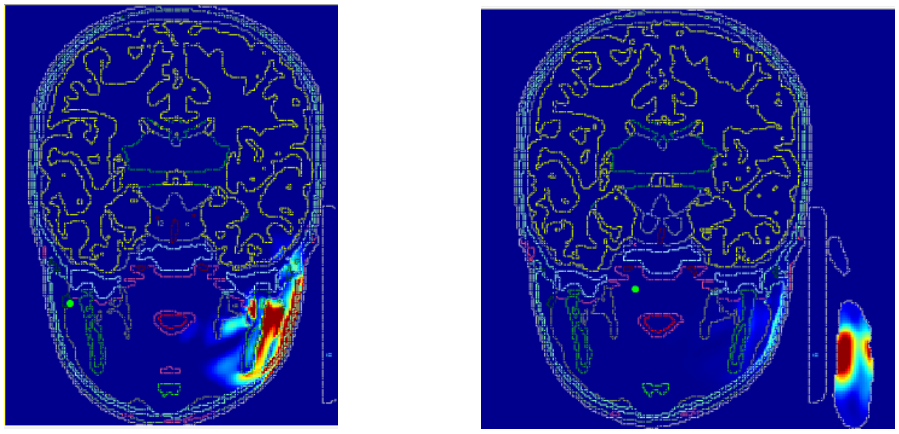

a) b)

Figure 5. SAR distribution inside the child head-hand models at 2100 MHz: a) head without hand, b) head and hand

Peak SAR location is observed inside the hand when the antenna is covered by the hand. Child hand absorbs a big part of the EM field energy and therefore, SAR peak values in the head tissues are reduced. It can be well seen from Figure 5.

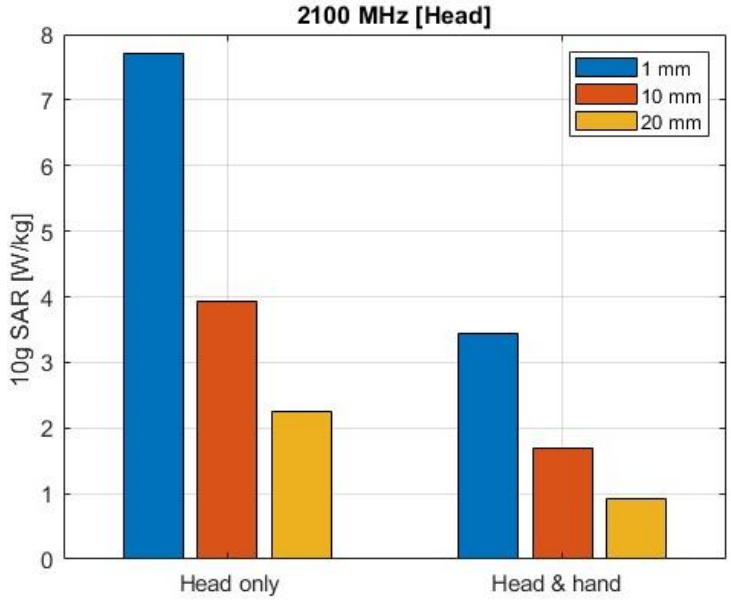

Figure 6. 10g SAR peak values for the child head model at 2100 MHz frequency.

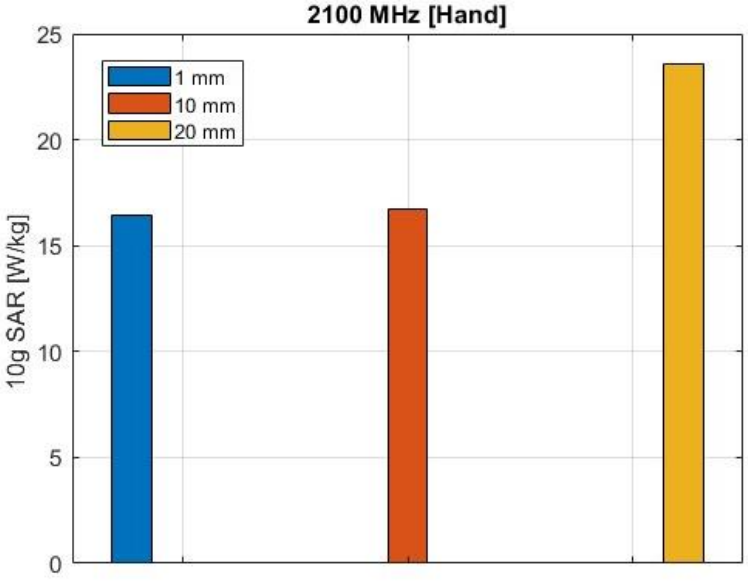

Figure 7. 10g SAR peak values for the child hand model at 2100 MHz frequency.

Due to the inverse dependence of the EM field on the square of the distance, the 10g SAR values are also inversely proportional to the distance between the mobile phone and child head. The 10g SAR value decreases when the distance between the child head model and the mobile phone is big. The peak SAR values in head tissues are reduced when the presence of the hand is taken into account (Figure 6 and Figure 7).

On Figure 8, dependence of SAR peak values on the matching conditions (S11 coefficient) is presented. SAR values are normalized to the value of the phone's EM field in free space. The first point on each graph corresponds to the value of SAR on the head without the hand, the second with the hand.

From the obtained results we can assume that bad matching is the reason for the increasing in peak SAR values in the child head and hand models. The hand, which holds the communication device, absorbs part of the radiated energy; therefore, to restore a good connection with the base station the total radiated power of the mobile phone increases. As a result, we obtain increased peak SAR values in the child head model.

4. CONCLUSION

The influence of a child's hand holding a mobile phone on the process of EM exposure was investigated in this paper. The research results showed that the presence of a hand changed the peak SAR values in the child's head model. The SAR values in the head model including the hand are lower than without the hand. Also, resultant SAR values reduce by increasing distance from the EM source to the child head.

It is clear that the selection of a model parameters affects the obtained results. The hand with which we hold the communication device absorbs part of the radiated energy; therefore, to establish a good connection with the base station, as already mentioned, the total radiated power of the mobile phone increases. As a result, the SAR peak increased values in the child head model are obtained.

It should be noted that the technological progress of communication devices is very fast, which makes it difficult to make general conclusions. For this reason, these problems are still relevant today and require further research.

REFERENCES

[1] [Online]. Available: IEEE Std (IEEE)., "Standard for Safety Level with Respect to Human Exposure to Radiofrequency Electromagnetic Fields, 3KHz to 300GHz", 2005.

[2] [Online]. Available: ICNIRP, "Guidelines for limiting exposure to time varying electric, magnetic and electromagnetic fields (up to 300 GHz),". Health Physics, vol. 74, pp. 494-522, April 1998.

[3] [Online]. Available: https://www.icnirp.org/en/activities/news/news-article/rf-guidelines-2020-published.html

[4] [Online]. Available: https://www.fcc.gov

[5] [Online]. Available: http://www.who.int/peh-emf/en/

[6] [Online]. Available:https://www.iarc.who.int/

[7] T. Nozadze, K. Henke, M. Kurtsikidze, V. Jeladze, G. Ghvedashvili, R. Zaridze. "Study How the Hand Affects on the MobileDipole Antenna Matching Conditions to the Free Space at 3700 MHz Frequency", 2022 IEEE 2nd Ukrainian Microwave Week, November 14th – 18th, 2022. DOI: 10.1109/UkrMW58013.2022.10037056

[8] V. Jeladze, T. Nozadze, I. Petoev-Darsavelidze & B. Partsvania, "Mobile phone antenna-matching study with different finger positions on an inhomogeneous human model", Electromagnetic Biology and Medicine, Volume 38, 2019 - Issue 4. 2019. DOI: 10.1080/15368378.2019.1641721

[9] T. Nozadze, V. Jeladze, R. Zaridze, 'Mobile Antenna Matching Study Considering Different Holding Positions at 2100 MHz Frequency', XXVIth International Seminar/Workshop on Direct and Inverse Problems of Electromagnetic and Acoustic Wave Theory DIPED-2020, Tbilisi, Georgia, September 15-18, 2020. DOI: 10.1109/DIPED49797.2020.9273363

[10] T. Nozadze, V. Jeladze, M. Tsverava, V. Tabatadze, M. Prishvin, R. Zaridze, "EM Exposure Study on an Inhomogeneous Child Model Considering Hand Effect", 2017 IEEE First Ukraine Conference on Electrical and Computer Engineering (UKRCON), Kyiv, Ukraine, May 29 -June 2, pp. 51, 2017. DOI: 10.1109/UKRCON.2017.8100484

[11] M. Abdul-Al, A. S. I. Amar, I. Elfergani, R. Littlehales, N. Ojaroudi Parchin, Y. Al-Yasir, Ch. Hwang See, D. Zhou, Z. Zainal Abidin, M. Alibakhshikenari, Ch. Zebiri, F. Elmegri, M. Abusitta, A. Ullah, F. M. A. Abdussalam, J. Rodriguez, N. J. McEwan, J. M. Noras, R. Hodgetts, R. A. Abd-Alhameed, "Wireless Electromagnetic

Radiation Assessment Based on the Specific Absorption Rate (SAR): A Review Case Study", Electronics 11(4), 511, 2022

[12] [Online]. Available: [Online]. https://itis.swiss/virtual-population/virtual-population/overview/

[13] [Online].Available:https://itis.swiss/virtualpopulation/tissueproperties/database/database-summary/)

APPLICATION OF FRACTAL METHODS TO THE ANALYSIS OF BIOCRYSTAL IMAGES

(selected from CEMA'23 Conference)

N. Ampilova[*] , V. Lyamin[*] and I. Soloviev[*]

[*] St. Petersburg State University, Comp. Sci. Dept

7/9 University emb., 199034 St. Petersburg, Russia

E-mail: n.ampilova@spbu.ru

Abstract

The analysis of digital images having complex structure includes the application both processing methods and mathematical algorithms. As a rule, the processing helps to find the representation of an image which is more suitable for application of mathematical methods. Depending on the type of images the obtaining of an appropriate presentation may be the essential part of the study. In the paper we apply the application of fractal and multifractal methods to compare crystals of medical preparations with a control image which does not contain a preparation (placebo). The images under study were prepared for analysis by a special program and transformed to grayscale palette. For several classes containing 5-6 images the applied methods demonstrated the separation of obtained characteristics, which means the difference in structures of medical preparations and placebo.

1. INTRODUCTION

In many cases digital images may be interpreted as phase portraits of complex processes in different moments of time. The analysis of these representations by mathematical methods gives a possibility to describe the properties of observed processes by using various characteristics (features) of the images.

As the distribution of pixel intensities is the main information about a digital image, specifications of the image are formulated in these terms. Many mathematical methods of analysis use a normed distribution on the cells of a given size, which is a probabilistic measure defined on the image. The choice of a measure may be performed by different ways depending on a problem. The simplest way takes the ratio of sum of pixel intensities in a cell to the common sum of intensities for the image. Such a method

results in an averaging of intensities, and sometimes smooths out the difference between parts of the image. The more preferable way is to take the ratio of the sum of intensities from a given interval (for a cell) to the sum of intensities from this interval for the image.

The experience of many researchers confirms that for images having complex structure the choice of appropriate methods is not just a technique, but an art. We should perform a filtration and improving the image quality, and not destroy its specific structure. This helps to highlight and emphasize certain properties of images and to facilitate their visual perception by an expert. In addition, the application of mathematical methods of analysis implies that the images under study are presented in a standard form convenient for solving the problems of a certain class. This work may be performed with the help of both graphic editors and specially devised programs.

In medical applications this approach furnishes insights into the clarification of the diagnosis. The combining filtration with following morphological analysis demonstrates reliable results in operating with radiograph and ultrasound images [3, 4].

Mathematical methods result in obtaining characteristic which may be used for further image classification. So, Haralick's texture methods describe the image structure in terms brightness ratio for neighboring pixels [5]. Morphological methods reveal specific patterns, for example contours of various forms [6].

Methods of fractal analysis describe the image by using fractal dimensions. As one numerical value cannot characterize the image structure, we should apply some modifications to obtain vector characteristics. In this sense, the "blanket technics" is very productive. It is applied to calculate the Minkovsky dimension for gray level images [2]. An image is represented as a surface in 3-dimension space, where two coordinates indicate the position of a pixel, and the third one is the pixel intensity. There is one-to-one correspondence between the surface and the given image. The surface is given by the gray level function, which is defined for integer values and then extended to real numbers. Such a definition corresponds to an approximation of the surface by unit squares parallel to the image plane.

Then we construct upper and bottom “blankets” for the surface by a definite rule, such that every next iteration is on the distance 1 from the previous one.

Actually, this procedure means a sequential smoothing of the surface. On every step we calculate the volume of the body between upper and bottom blankets and then calculate an approximate value of the surface area and as a result the Minkovsky dimension of the surface. However, the most informative characteristic is not this dimension, but the ratio logarithm of the area on the next step to the logarithm of the step number. For a given set of steps we obtain a vector value (called further by characteristic vector). These vectors are different for images of different classes.

Blanket technics was successfully applied for study of biomedical preparations [1] and SAR images as well [8,9].

Multifractal methods are useful if analyzed images may be interpreted as a union of several fractal subsets. In this case we can obtain the set of fractal dimensions of the subsets (multifractal spectrum) or Renyi spectra measuring changes of the initial distribution of pixel intensities at its sequential renormalizations.

Our experience when analyzing biomedical images allows proposing a combined application of fractal and multifractal methods to obtain reliable results [10].

In this work we developed a technology for differentiation crystals of medical preparations obtained by the thesiography method from the image of control pattern which does not contain the preparation. The preprocessing included editing of images from a microscope by a special program followed by filtration and transformation to halftone representation. Mathematical methods used in this paper are calculation of characteristic vector (blanket technics) and Renyi spectra. Experiments were performed for 3 classes of medical preparation images. All the results demonstrated the separation of calculated features.

The paper has the following structure. The next section contains the description of material and methods to obtain images. In section 3 we briefly describe the preliminary processing of the images from a microscope for the application of mathematical methods. The next part is devoted to the fractal and multifractal methods. The results of experiments are demonstrated in section 5.

2. MATERIAL AND METHODS

2.1. Materials

The images were obtained by the light microscope MIKMED – 6, which consists of eyepiece LOMO WF 10X/22, objectives Plan 4/0,1 Plan 10/0,25 Plan 40/0,65, and video-camera MC – 6,3 (USB-3,0).

The samples were prepared on laboratory slides. Medical preparations of plant, animal and mineral origin in dilution from 1 to 1000 CH by C. Haneman were manufactured in pharmacy POLEVET (oil). Sterile brine solution (NaCl – 0.9%) was used.

2. 2. Method of studying

The research of the crystallization of biosubstrates was conducted by thesiograthy method. At first the preparation under study was dynamized (by the method of "shaking"). Brine solution (from 1 to 3 drop depending on the substrate quantity) was dripped on a slide. Then 1 drop of the substrate was set in the drop of brine solution. The result of crystallization was fixed after 24 hours. The image of brine solution (placebo) was taken as the control one. The obtained crystals of biosubstrates were compared with the control image.

3. IMAGE EDITING

3.1. Transformation of images to a standard form

To apply methods of image analysis we should convert the images to some appropriate form. For this purpose we cut out the part of the image which contains crystal. The cutting is produced so that there was a "little" space between crystal and the image boundary. One may use graphic editors such as Gravit Designer, Photo Pos Pro, Paint. It is important to do it so the center of the crystal coincide with the center of the image. Then, following the formula below, we perform a rotation of the image so that the sides of the crystal faces become parallel to the sides of the image.

$$x_1 = x_0 + (x - \mathrm{w}/2)\cos\varphi - (y - \mathrm{h}/2)sin\varphi$$

$$y_1 = x_0 + (x - \mathrm{w}/2)\sin\varphi - (y - \mathrm{h}/2)cos\varphi$$

where (x_1, y_1) — new coordinates, (x,y) — old coordinates, (x_0, y_0) the center of rotation, and ϕ — the angle of rotation, and (w,h) define the size of the new image. This

transformation is performed by a C# program. After the processing of initial images by the described way we choose the image of minimal size and cut all the others by this size. Then all the images are transformed to grayscale palette. The illustrating example is given below.

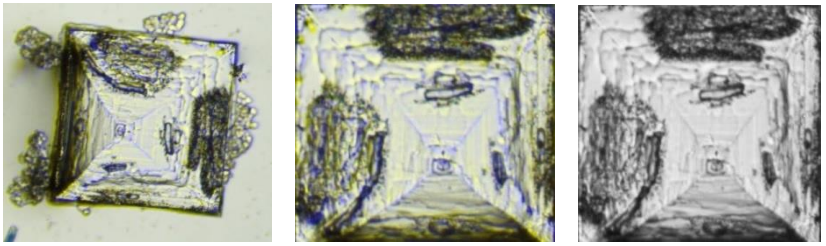

a b c

Figure 1. a) a crystal, b) after rotation and cutting,c) grayscale image

3.2. Image preprocessing

We considered global and local equalization, the Laplace operator, linear and nonlinear filtering, unsharp masking.. The experiments show that global and local equalization practically did not give expected results, as well as filtering. So we applied the Laplace operator and unsharp masking. The first method is isotropic, i.e. invariant under rotation, and unsharp masking allows flexible parametric adjustment.

4. MATHEMATICAL METHODS

4.1. Blanket construction

A detailed description of this method can be found in [2, 11], so we will provide here only the information necessary to describe the algorithm of implementation.

Let $\mathrm{G} = \{\mathrm{X_{ij}}, \mathrm{i} = 0,1, \ldots, \mathrm{K}, \mathrm{j} = 0,1, \ldots, \mathrm{L}\}$ be a gray-scale image and X_{ij} be the gray level of the (i, j)-th pixel. This is a gray-level surface for the image, which can be viewed as a fractal for a certain measure range.

Consider $F \subset \mathbb{R}^n$. Then δ-parallel body F_δ is a set of points being at the distance of no more than δ from F, i.e

$$F_\delta = \{x \in \mathbb{R}^n : |x - y| \leq \delta, y \in F\}.$$

We denote by $Vol(F_\delta)$ n-dimensional volume of F_δ. If for some constant s at the limit $Vol(F_\delta)/\delta^{n-D}$ $\delta \to 0$ is positive and bounded, then the number D is called the Minkovski dimension of the set F.

Blankets u_δ, b_δ for a gray level surface are constructed as follows

$$u_\delta(i,j) = max\ \{u_{\delta-1}(i,j) + 1, \quad \max_{|(m,n)-(i,j)|\le 1} u_{\delta-1}(m,n)\}$$
$$b_\delta(i,j) = min\ \{b_{\delta-1}(i,j) - 1, \quad \min_{|(m,n)-(i,j)|\le 1} u_{\delta-1}(m,n)\}$$
$$u_0(i,j) = b_0(i,j) = X_{ij}$$

A point $F(x,y)$ is included in a δ-parallel body if $b_\delta(i,j) < F(x,y) < u_\delta(i,j)$. The definition of a blanket is based on the fact that the blanket for a surface on the step δ includes all the points of the blanket for a surface constructed on the step $\delta - 1$ together with the points that are at the distance of 1 from this blanket.

The volume of a δ-parallel body is calculated by u_δ and b_δ:

$$Vol(F_\delta) = \sum_{i,j}(u_\delta(i,j) - b_\delta(i,j)).$$

The surface area may be calculated using one of two formulas

$$A_\delta = \frac{Vol_\delta}{2\delta}$$

$$A_\delta = \frac{Vol_\delta - Vol_{\delta-1}}{2}.$$

The Minkovsky dimension is defined as $D \approx 2 - \frac{\ln A_\delta}{\ln \delta}$

To obtain the image characteristics, we use a vector $\{(\ln \delta, \ln A_\delta)\}$, the size of which is determined by the number of different values of δ.

4.2. Renyi spectra

The detailed information about multifractal and Renyi spectra may be found in [6]. Consider the set $M \subset R^n$, and its partition into $N(\varepsilon)$ cells with side (or volume) ε. We define the probability measure $p(\varepsilon) = \{p_i(\varepsilon)\}$, $i = 1, \dots, N(\varepsilon)$, $\sum_{i=1}^{N(\varepsilon)} p_i(\varepsilon) = 1$.

Also consider the generalized statistical sum (or the sum of the moments of the measure)

$$S(q,\varepsilon) = \sum_{i=1}^{N(\varepsilon)} p_i^q(\varepsilon)$$

As usual in multifractal technique we assume that for the measure and statistical sum the power law holds:

$$p_i(\varepsilon) \sim \varepsilon^{\alpha_i}, \quad S(q,\varepsilon) \sim \varepsilon^{\tau(q)}$$

where $\tau(q)$ is a function of class C^1. The symbol "~" is understood as follows:

$$\alpha_i = \lim_{\varepsilon \to 0} \frac{\ln p_i(\varepsilon)}{\ln \varepsilon}, \tau(q) = \lim_{\varepsilon \to 0} \frac{\ln S(q,\varepsilon)}{\ln \varepsilon}.$$

Under these assumptions, the set of generalized Renyi dimensions is defined as

$$D_q = \lim_{\varepsilon \to 0} \frac{1}{q-1} \frac{\ln S(q,\varepsilon)}{\ln \varepsilon}$$

These values describe the changing of initial measure $\{p_i(\varepsilon)\}$ for a range of q.

For q=0 we obtain capacity dimension, and for q=1 by applying the Lopital rule -- the so called information dimension (or the dimension of a measure support)

$$D_1 = \lim_{\varepsilon \to 0} \frac{\sum_i p_i(\varepsilon) \ln p_i(\varepsilon)}{\ln \varepsilon}.$$

5. RESULTS OF EXPERIMENTS

In all the illustrations we use following denotations

Table 1. The correspondence between preparation used and their denotation in graphs

Preparation	Denotation
Placebo (brine solution)	Sample 0
Conium 1000 CH	Sample 1
Acidum phosphoricum 30 CH	Sample 2
Lac defloratum 1000 CH	Sample 3

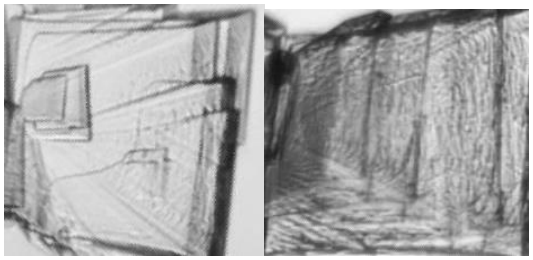

a b

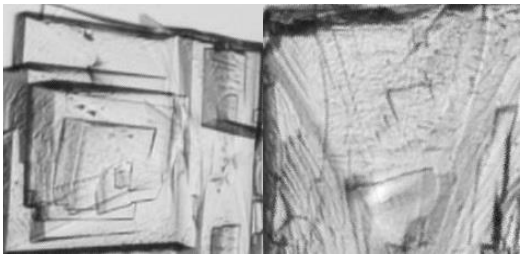

c d

Figure 2. a) Sample 0, b) Sample 1, c) Sample 2, d) Sample 3

The picture shows images of crystals of biosubstrates and placebo. On Fig.3 graphs of characteristic vectors and Renyi spectra for Sample 1 and Sample 0 are given. Graphs are separated. The point of intersection in Renyi spectra (q=0) means that all the images have close value of capacity dimension.

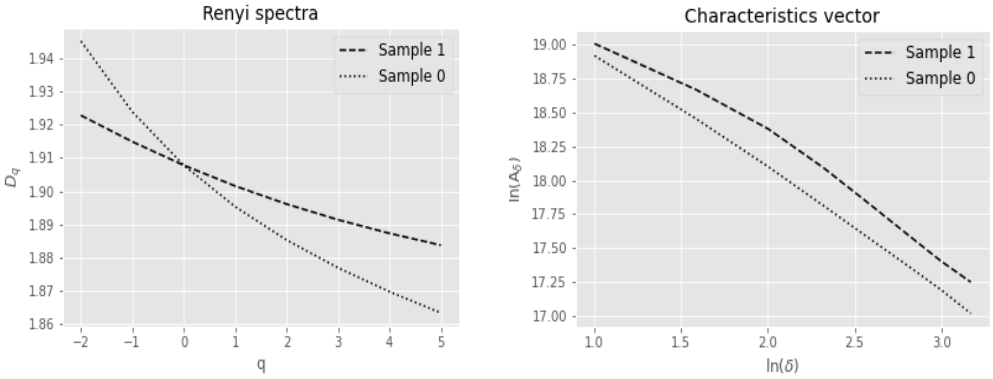

Figure 3 Comparing results for Conium 1000 CH and Placebo a) Renyi spectra and b) characteristic vectors

The following graphs demonstrate the difference between the structure of the crystal of *Acidum* phosphoricum 30 CH and placebo.

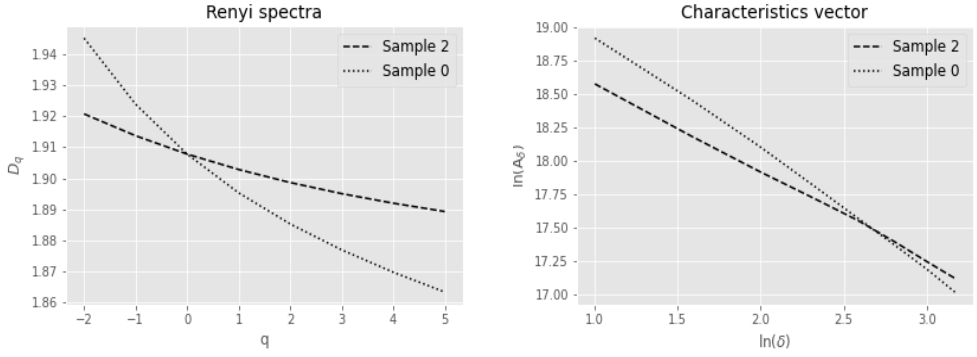

Figure 4. Comparing results for *Acidum* phosphoricum 30 CH and placebo a) Renyi spectra and b) characteristic vectors

In this case, Renyi spectra give a better result than characteristic vectors. Analogical graphs for the crystals of Lac defloratum 1000 CH and placebo are given in Fig.5.

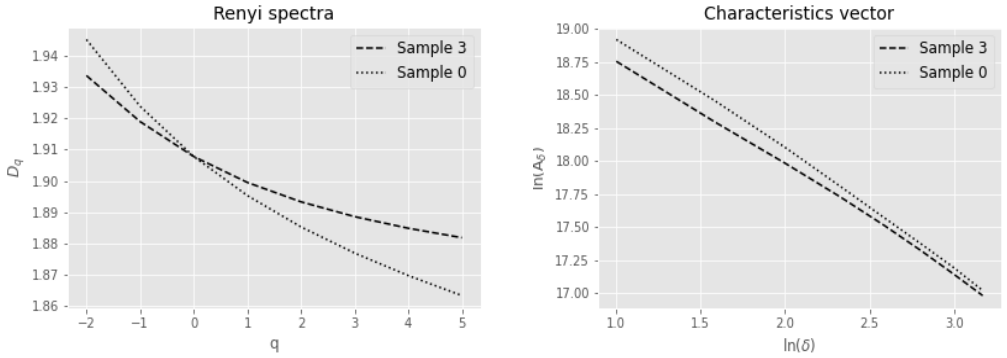

Figure.5. Comparing results for Lac defloratum 1000 CH and placebo

6. CONCLUSION

Our experiments show that the combining of an appropriate image preprocessing and methods of fractal analysis allows obtaining graphs that are separated.

The fact that Renyi spectra have a point of intersection near q=0 means that all the images studied have close values of capacity dimension. Hence to obtain classifying signs one need to use vector characteristics.

REFERENCES

[1] N. Ampilova, I. Soloviev , J.-G. Barth. “Application of fractal analysis methods to images obtained by crystallization modified by an additive”. Journal of Measurements in Engineering, Vol. 7, Issue 2, 2019, p. 48-5https://doi.org/10.21595/jme.2019.20436

[2] K. J. Falconer, "Fractal geometry", Chichester : Wiley,1990.

[3] V.Georgieva, S. Vassilev. “Kidney segmentation in ultrasound images via active countours”, Proc. 11 Int. Conf. CEMA16, 13-15 Oct. 2016, Sofia, Bulgaria. p.43-46

[4] V. Geogieva, P.Petrov, B.Iantovics. “X-ray image processing for tissue involvent-based caries detection”, Proc. 14 Int. Conf. CEMA19, 17-19 Oct. 2017, Sofia, Bulgaria. p.22-26.

[5] R. M. Haralick, K. Shanmugan, I. Dinstein. "Textural Features for Image Classification", IEEE Transactions on systems, man and cybernetics, volume SMC-3. - IEEE, 1979. - №6. - P. 610-621. - ISSN 00189472.

[6] R. Gonzalez, R Woods. "Digital image processing", 2002

[7] S.P. Kuznetsov, "Dynamical chaos", M, Izd.fiz-mat lit.,2001 (in Russian)

[8] A. Malamou, C.Pandis, P.Frangos and P. Stefaness. "SAR image terrain classification using the modified fractal signature (MFS) method", Proc. 9 Int. Conf. CEMA14, 16-18 Oct. 2014, Sofia, Bulgaria. p.8-11.

[9] G. Pouraimis, A. Kotopoulis, N. Ampilova, I. Soloviev, E. Kalitsis and P. Frangos, "Sea state determination using normalized one-dimensional radar signatures at X-band and fractal techiques", Proc. 14 Int. Conf. CEMA19, 17-19 Oct. 2019, Sofia, Bulgaria, p. 27-31.

[10] I. Soloviev, "Application of multifractal methods for the analysis of crystal structures", JAE 2022, JAE-Journal of Applied Electromagnetism /http:///jae.ece.ntua.gr), 24(2),19-30.

[11] Y. Y. Tang, C. Y. Suen, "Modified fractal signature (MFS): a new approach to document analysis for automatic knowledge acquisition", IEEE Transactions on Knowledge and Data Engineering,1997, 9, № 5,p. 747-762.